Electronic Supplementary Material (ESI) for Journal of Materials Chemistry A.
This journal is © The Royal Society of Chemistry 2021

Electronic Supporting Information

General Surface Grafting Strategy Derived Carbon Modified Graphitic Carbon Nitride with Largely Enhanced Visible Light Photocatalytic H_2 Evolution Coupled with Benzyl Alchol Oxidation

Haifei Wang[#], Jihua Zhang[#], Xu Jin[#], Xiaoqi Wang, Fu Zhang, Jierui Xue, Yapeng Li, Jianming Li* and Genqiang Zhang*

Mr. H. F. Wang, Mr. F. Zhang, Mr. J. R. Xue, Mr. Y. P. Li, and Prof. G. Q. Zhang
Hefei National Laboratory for Physical Sciences at the Microscale, CAS Key Laboratory of Materials for Energy Conversion, Department of Materials Science and Engineering, University of Science and Technology of China, Hefei, Anhui 230026, China

Dr. J. M. Li, Dr. X. Jin and Dr. X. Q. Wang
Research Institute of Petroleum Exploration & Development (RIPED), PetroChina, Beijing, 100083, China

Dr. J. H. Zhang
Guizhou Provincial Key Laboratory of Computational Nano-Material Science, Guizhou Education University, Guiyang, Guizhou 550018, China

[#] These authors contribute equally to this work.

[*] To whom the correspondence should be referred. Email: gqzhangmse@ustc.edu.cn

Email: lijm02@petrochina.com.cn

1. Experimental Procedures

1.1 Materials

Melamine, p-phenylene diisocyanate (PPDI), and dichloromethane (CH_2Cl_2) were purchased from Aladdin Industrial Corporation and and used without further purification.

1.2 The synthesis of pure carbon nitride (MCN):

The g-C_3N_4 was synthesized by heating 3 g melamine in a muffle furnace at 550 ^oC for 4 h at the air atmosphere with a heating rate of 2 ^oC min^{-1}. After cooled down to room temperature, the final yellow product was grinded into powder and dispersed in deionized water, and sonicated for 2 h. Then the dispersion was centrifuged and dried at 80 ^oC overnight. The final product was marked as MCN. The UCN was synthesized by the same method using urea as the precursor.

1.3 The synthesis of carbon modified carbon nitride (CMCN-x and CUCN-x):

0.2 g MCN was dispersed in 40 mL DMF by sonication. Then the amount of p-phenylene diisocyanate (PPDI) was added into the suspension of MCN and sonicated for 1.5 h to ensure the uniform dispersion, the dispersion was stirred at 60 ^oC for 24 h. The reaction mixture was separated by centrifugation and washed with dichloromethane to remove the residual species. After dried at 80 ^oC overnight, the sample was transferred into an alumina crucible with a cover and wrapped with tin foil slightly, and calcined at 500 ^oC for 2 h under Ar atmosphere using a heating rate of 2 ^oC min^{-1}. The final obtained products are labeled as CMCN-x (x = 0.5, 1, 2, 5), the x wt% is the percentage of PPDI to MCN. Replacing MCN with UCN, the CUCN was prepared by the same method and marked as CUCN-x, while the x wt% is the percentage of PPDI to UCN.

1.4 The synthesis of carbon modified carbon nitride treated at different temperatures (CMCN-y °C):

Except the in-situ carbonization temperature, all processes keep the same with the preparation of CMCN-1. The samples synthesized under different temperatures are named as CMCN-y, where y is equal to 450, 500, 550, and 600, representing the treating temperature.

1.5 The synthesis of carbon materials by carbonized PPDI directly:

The crbon martials are developed by directly calcining PPDI under Ar atmosphere using a heating rate of 2 °C min^{-1} for 2 h at the temperatures of 450, 500, 550, and 600 °C, and simply noted as 4450, 500, 550, and 600. Besides, carbonized PPDI means the sample directly carbonized PPDI at 500 °C for 2 h.

2. Characterizations:

The morphology and structure of the as-prepared samples were observed by scanning electron microscope (SEM) and transmission electron microscopy (TEM). The SEM images were obtained with a field-emission microscope by a FEI SU8220. Transmission electron microscopy (TEM) images, high-angle annular dark-field scanning transmission electron microscopy (HAADF-STEM) were collected with a Talox F200X (Thermo Fisher Scientific, America) transmission electron microscope operating at 200 kV. The crystalline structures were analyzed by X-ray diffraction (XRD) using a Cu Kα source (TTR-III, Rigaku Industrial Corporation, Japan). Fourier transform infrared spectroscopy (FTIR) was performed with a Nicolet 8700 spectrometer (Thermo Nicolet Corporation, America) using KBr pallets. X-ray photoelectron spectroscopy (XPS) was carried out on an ESCA Lab 250 X-ray photoelectron spectrometer (Thermo-VG Scientific, America). The XPS peak of carbon (C1s whose binding energy is 284.6 eV) was used to eliminate the effect of surface charging of the sample. Time-resolved photoluminescence (TRPL) curves were acquired using a time-corrected single-photon counting (TCSPC) system (FM4-TCSPC, Horiba Jobin Yvon) with an excitation wavelength of 436 nm. Photoluminescence (PL) was measured on an F-4600 FL spectrophotometer (Hitachi Ltd., Japan) with an excited wavelength 350 nm. UV-Visible absorption spectroscopy was obtained from the SOLID3700 ultraviolet-visible light spectrophotometer (Shimadzu Corporation, Japan). The electron paramagnetic resonance spectra was collected using JES-FA200 (JEOL, Japan). Solid-state ^{13}C MAS NMR spectra are operated on Bruker AVANCE NEO 600 WB.

3. Electrochemical measurement:

Electrochemical measurements were conducted with a CH Instruments 760E Electrochemical System in a conventional three electrode cell using Pt sheet, FTO coated with catalysts, and Ag/AgCl as the counter electrode, working electrode, and reference electrode, respectively. The details of the preparation of working electrodes were as follows: 5 mg catalyst was dispersed in 2 mL PTFE aqueous solution (0.4 g L^{-1}) by sonication. Then, 10 μL the dispersion was drop-coated at 1 × 3 cm^2 FTO glass with a coated area of 1 × 1 cm^2. The FOT glasses were dried at 80 ^{o}C for 24 h before using. 0.5 M Na_2SO_4 served as the electrolyte. Photocurrent measurement utilized a 300 W Xe lamp equipped with a 420 nm cutoff filter. In order to minimize absorption by the thick catalyst layer, the working electrode was back-illuminated through the FTO glass. The impedance-potential curve was performed to obtain Mott-Schottky plots for working electrodes at potential windows ranged from -1 to +1 V with a frequency of 1.0, 1.5, and 2.0 kHz, respectively. The EIS measurements were performed by applying an AC voltage with 5 mV amplitude with the frequency range of 0.01 Hz to 100 kHz under open circuit potential conditions.

4. Photocatalytic tests:

The photocatalytic hydrogen evolution experiments were carried out in an online photocatalytic hydrogen production system (Lasolar-6A, Beijing PerfectLight Co. Ltd, China) using a top-irradiation-type Pyrex reaction cell (total volume of 150 mL with a top irradiation area of 15.9 cm^2). A 300 W xenon lamp (PLS-SXE 300, Beijing PerfectLight Co. Ltd, China) was used as the light source with a 420 nm cutoff filter for visible light (420 nm $\leq \lambda \leq$ 780 nm) or a standard AM1.5 filter for full-spectrum (ca. 100 mW cm^{-2}). The 10 mg sample was dispersed in 20 mL aqueous solution with 10 vol% triethanolamine and 0.210 mL 1 g L^{-1} H_2PtCl_6 (1 wt% Pt as the co-catalyst, by in situ photo-deposition). Before irradiated under a 300 W Xe lamp with a 420 nm cutoff filter, the reactor was sealed and evacuated several times to remove air. The reaction solution temperature was controlled at 5 ^{o}C by a flow of cooling water throughout the reaction. The generated hydrogen was analyzed by on-line gas chromatography (GC 7900, Techcomp, China) equipped with a thermal conduction detector using high-purity Ar as the carrier gas. The 3 cycles with a time interval of 12 hours were performed. The different wavelength was obtained by 300 W Xe lamps with a bandpass filter of 420, 450 and 500 nm, and the intensity was 14.5, 14.3, and 32.9 mW cm^{-2}, respectively. Simultaneous oxidation of benzyl alcohol and hydrogen evolution was carried out by using benzyl alcohol as the sacrificial agency. Typically, 20 mg as a prepared photocatalyst was dispersed in 80 mL aqueous solution with 0.420 mL 1 g L^{-1} H_2PtCl_6. After the irradiation under a 300 W Xe lamp with a standard AM1.5 filter for 30 mins, 800 μmol benzyl alcohol was added into the reaction solution. Before irradiated under a 300 W Xe lamp with a 420 nm cutoff filter, the reactor was sealed and evacuated several times to remove air. The reaction solution temperature was controlled at 5 ^{o}C by a flow of cooling water throughout the reaction. The generated hydrogen was analyzed by on-line gas chromatography (GC 7900, Techcomp, China) equipped with a thermal conduction detector using high-purity Ar as the carrier gas. When the reaction finished, the resultant solution was centrifuged and the supernatant was extracted with 3 × 10 mL CH_2Cl_2 and dried with anhydrous Na_2SO_4. The product was analyzed and quantified by gas chromatography (Agilent 7890B, N_2 as the carrier gas, Flame Ionization Detector).

The Apparent Quantum Efficiency (AQE) was measured at a different wavelength (420, 450, and 500 nm, $\lambda \pm 10$ nm) in a 300 W Xe lamp with the total irradiation power of 88.7, 71.1, and 178.9 mW. The incident photons (N_e) is calculated by equation (1). The AQE was calculated by equation (2).

$$N_e = E\lambda/hc \qquad (1)$$

E is the intensity of incident light, λ is the wavelength, h is the Planck constant,, c is the speed of light.

$$AQE = 2MN_A/N_e{*}100\% \qquad (2)$$

M is the amount of H_2 molecules, N_A is Avogadro constant.

5. DFT calculation details:

Density functional theory (DFT) based first-principles calculations are performed using the projected augmented wave (PAW)[1] method implemented in the Vienna *ab initio* simulation package (VASP).[2, 3] The Kohn-Sham one-electron states are expanded using the plane-wave basis set with a kinetic energy cutoff of 400 eV. The Perdew-Burke-Ernzerhof (PBE) exchange-correlation potential within the generalized gradient approximation (GGA) is employed for the geometric optimizations and electronic structure calculations.[4] The Monkhorst–Pack[5] k-point mesh of 2 × 2 × 1 was used to perform geometry optimizations, and 4 × 4 × 1 k-point mesh was used for the electronic structure calculations, respectively. All atoms were relaxed until the Hellman-Feynman forces on individual atoms are less than 0.01 eV $Å^{-1}$. The vacuum thickness along the z-axis was set to 20 Å, which is large enough to prevent interaction between adjacent layers. To study the adsorption of graphene on the g-C_3N_4 involved in photocatalytic splitting of water, we have considered a six-carbon-ring of graphene adsorbed to 3 × 3 ×1 supercell of the g-C_3N_4 with 54 carbon atoms and 72 nitrogen atoms.

6. Results and discussion:

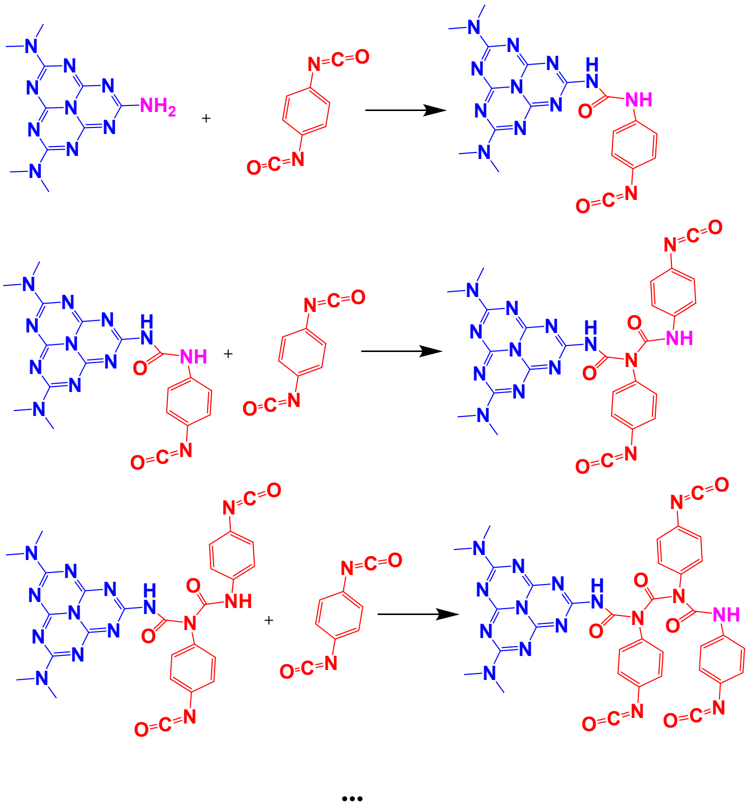

Figure S1. The process of grafting reaction between PPDI and MCN.

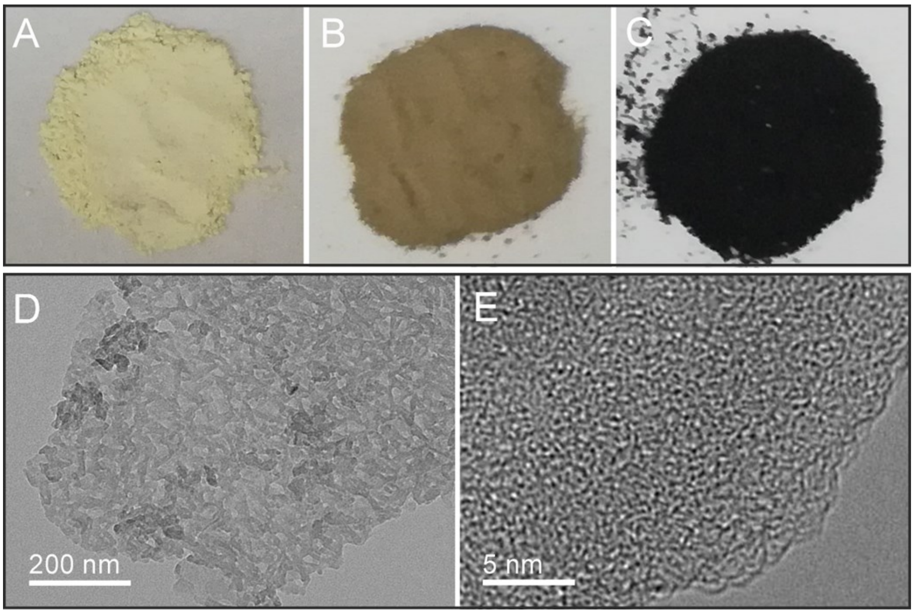

Figure S2. The sample photographs of (A) MCN; (B) CMCN-1; (C) calcined PPDI under the same condition; (D) and (E) the TEM and HRTEM images of MCN, respectively.

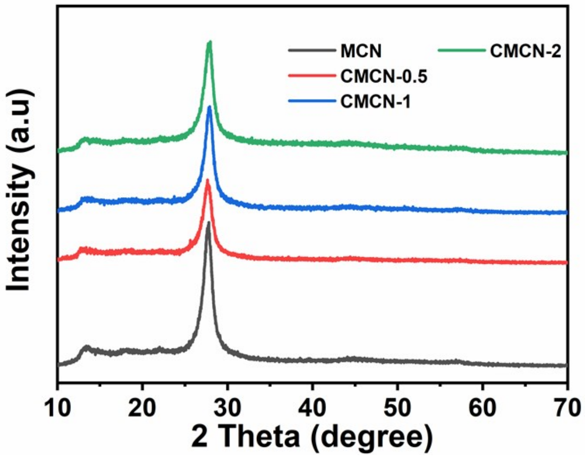

Figure S3. The XRD patterns of different samples.

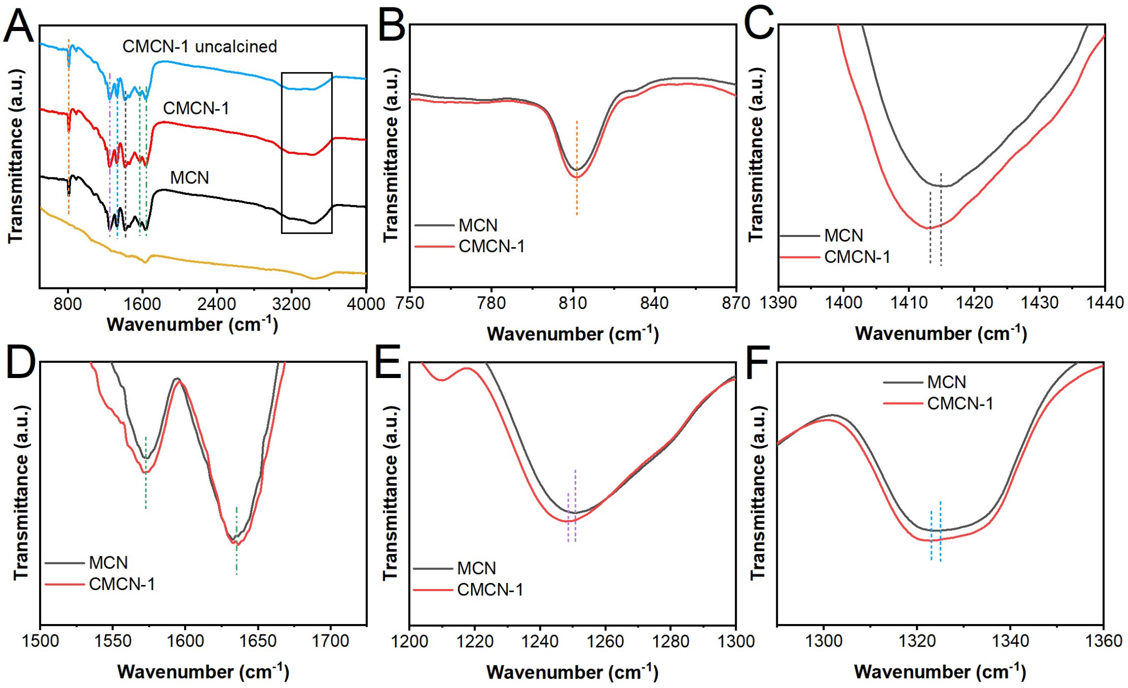

Figure S4. The FTIR spectra of different samples.

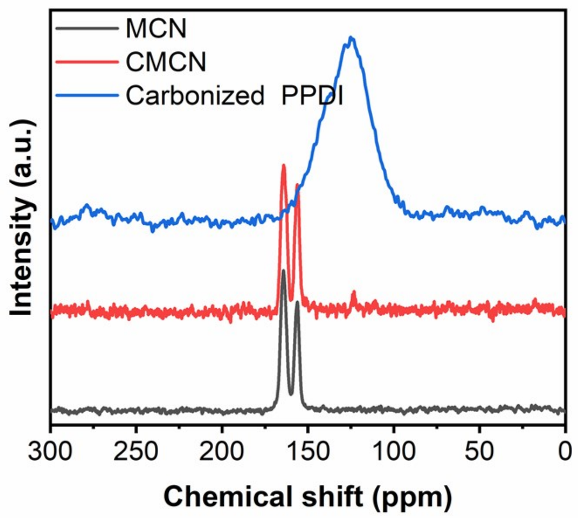

Figure S5. Solid-state ^{13}C MAS NMR spectra of MCN, CMCN-1, and carbonized PPDI.

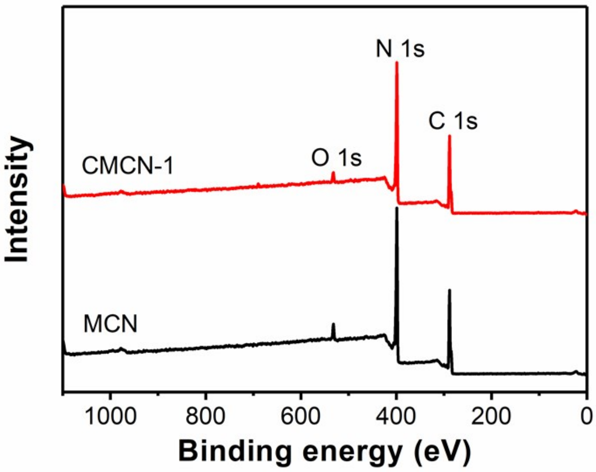

Figure S6. The XPS spectra of MCN and CMCN-1

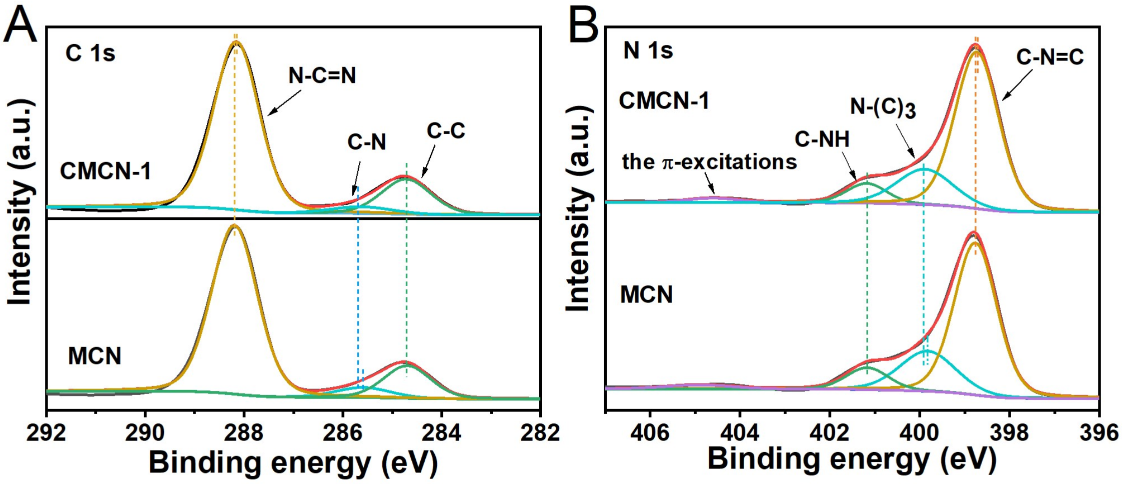

Figure S7. (A) The C 1s XPS spectra, and (B) N 1s XPS spectra of MCN and CMCN-1.

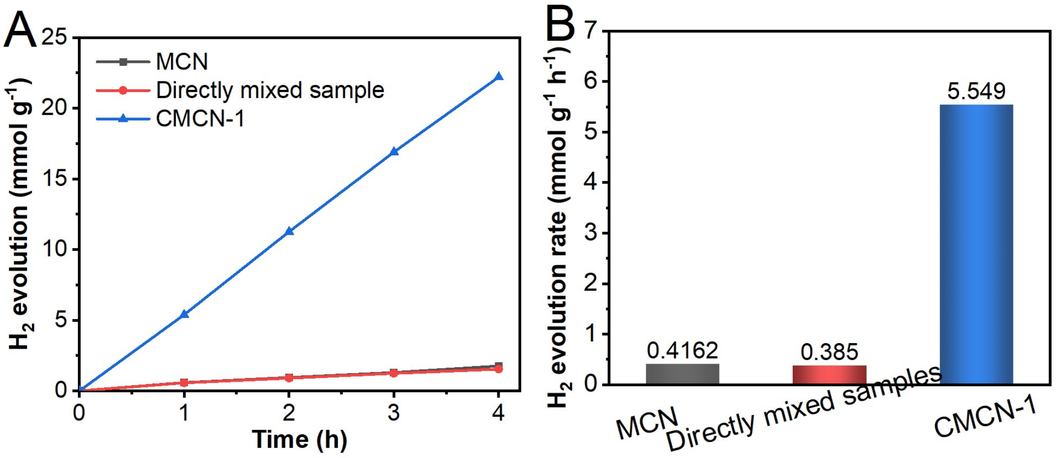

Figure S8. The photocatalytic performance of MCN, Directly mixed samples, and CMCN-1 under visible light irradiation.

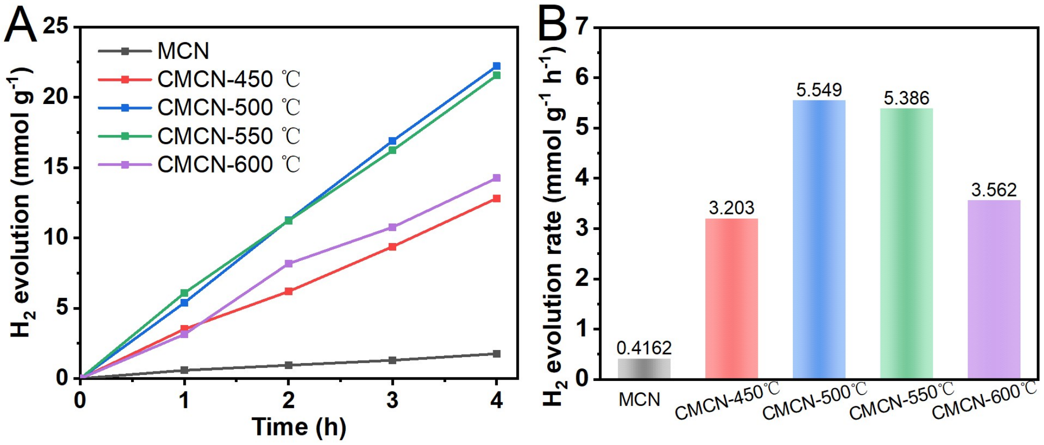

Figure S9. The photocatalytic performance of MCN and CMCN treated under different temperatures.

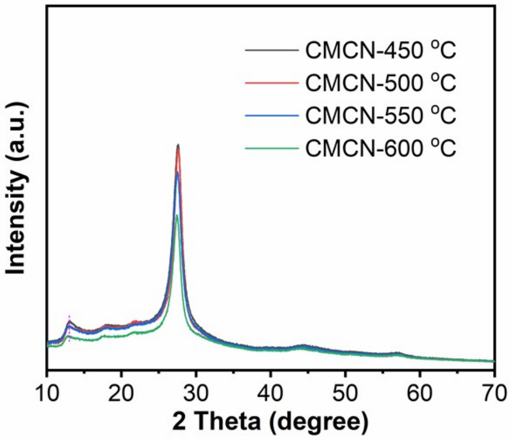

Figure S10. XRD patterns of CMCN-1 treated at different temperatures.

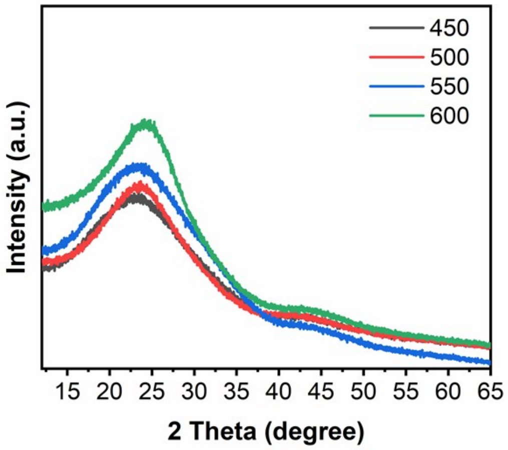

Figure S11. The XRD patterns of the carbon materials of carbonized PPDI at the temperatures of 450 °C, 500 °C, 550 °C, and 600 °C, respectively.

As seen in **Fig. S11**, one broad peak at about 24.5° attributed to the (002) crystal plane of graphite can be observed for all samples treated at the temperature from 450 to 600 °C, and the intensity increases with the treating temperature, revealing that graphitization intensified with the temperature being higher. This result can be further proved by the Raman spectra **Fig. S12**.

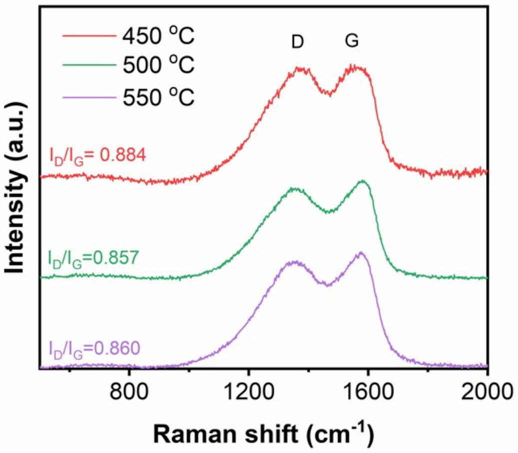

Figure S12. Raman results of the carbon materials of carbonized PPDI at the temperatures of 450 °C, 500 °C, and 550 °C, respectively.

Raman spectra show two peaks centered at 1372 and 1572 cm^{-1}, which were attributed to induced D band and vibrational G- band, respectively. More importantly, the value of I_D/I_G decreased with the temperature being higher, suggesting that less defects exist. The low graphitization with more defects may accounts for the relatively low photocatalytic performance of CMCN-450 °C when compared to CMCN-500 °C and CMCN-550 °C (**Fig. S9**)

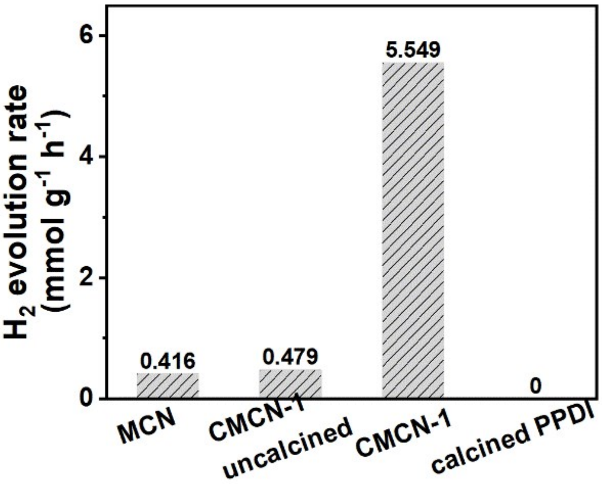

Figure S13. H_2 evolution rates of MCN, CMCN-1, CMCN-1 uncalcined, and calcined PPDI under visible light irradiation under visible light irradiation.

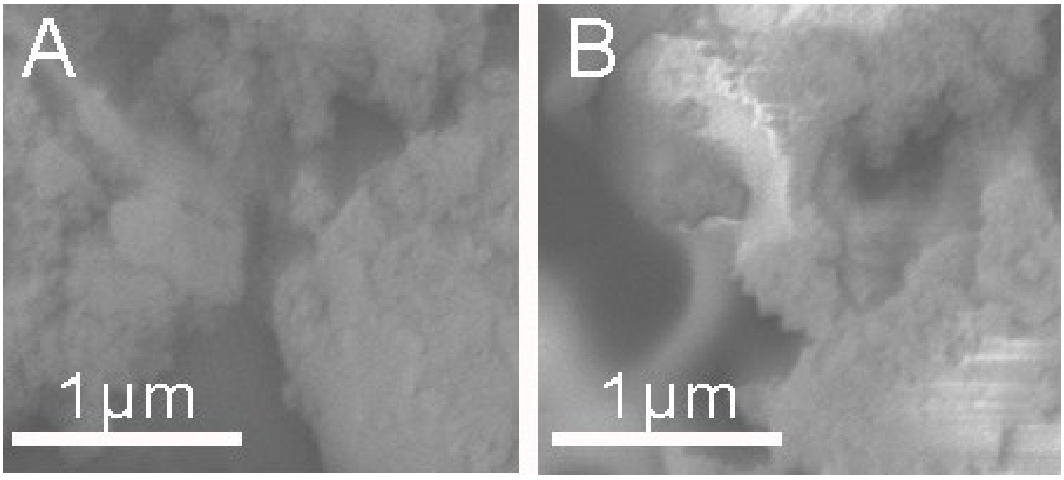

Figure S14. The SEM images of of CMCM-1 before (A) and after (B) recycling photocatalytic experiment.

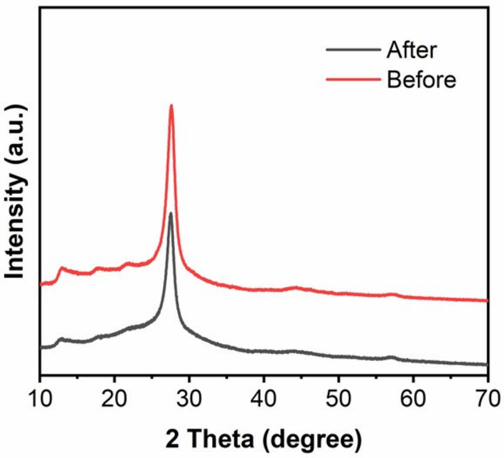

Figure S15. The XRD patterns of CMCM-1 before and after recycling photocatalytic experiment.

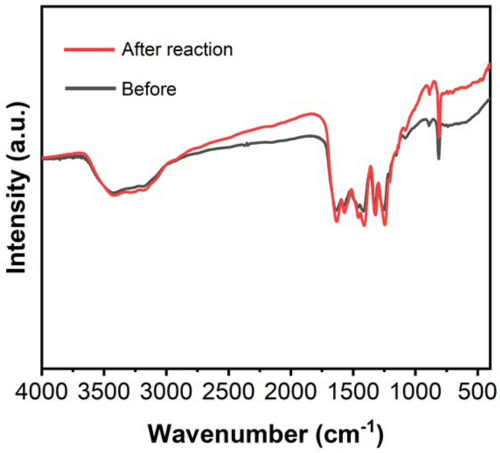

Figure S16. The FT-IR spectra of CMCM-1 before and after recycling photocatalytic experiment.

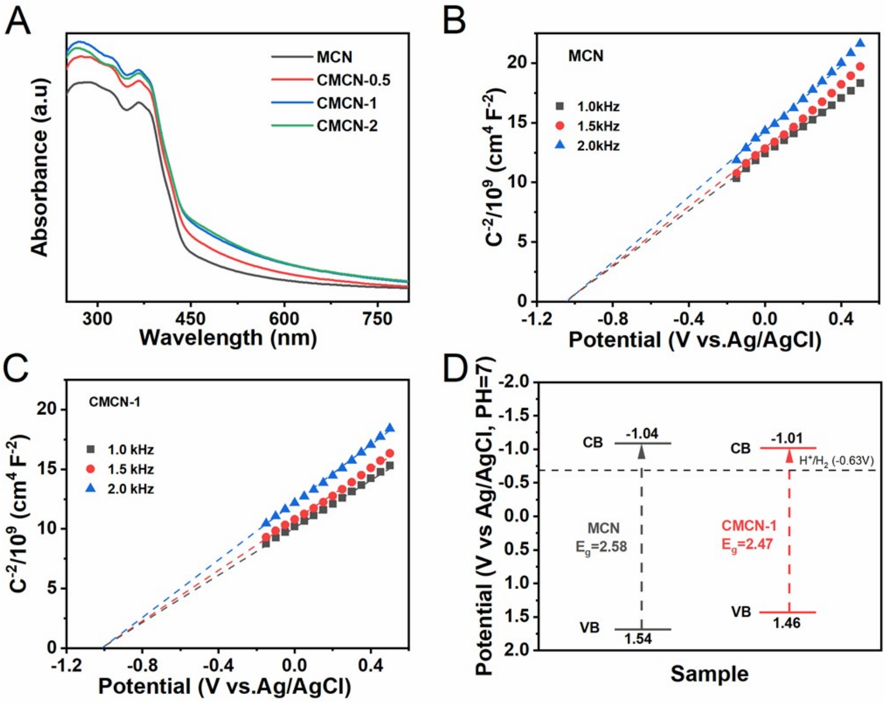

Figure S17. (A) UV-Vis diffuse reflectance spectra for different samples; (B,C) the Mott-Shottky plots of MCN and CMCN-1, respectively; (D) the band structures of MCN and CMCN-1.

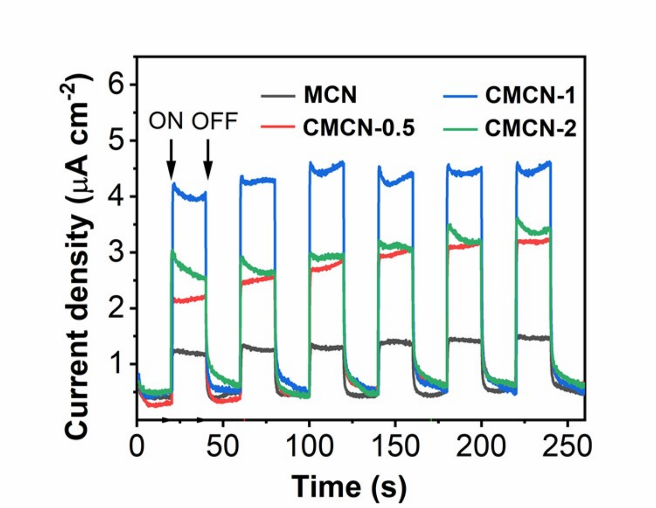

Figure S18. Transient photocurrent response curves for MCN and CMCN-0.5, CMCN-1, and CMCN-2.

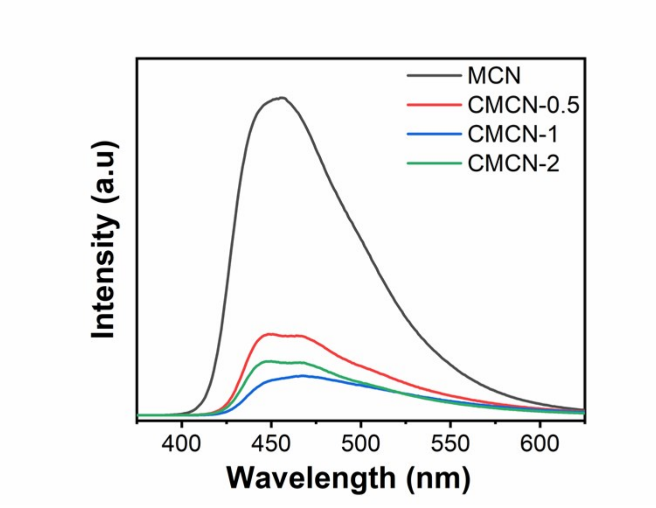

Figure S19. PL spectra for MCN and CMCN.

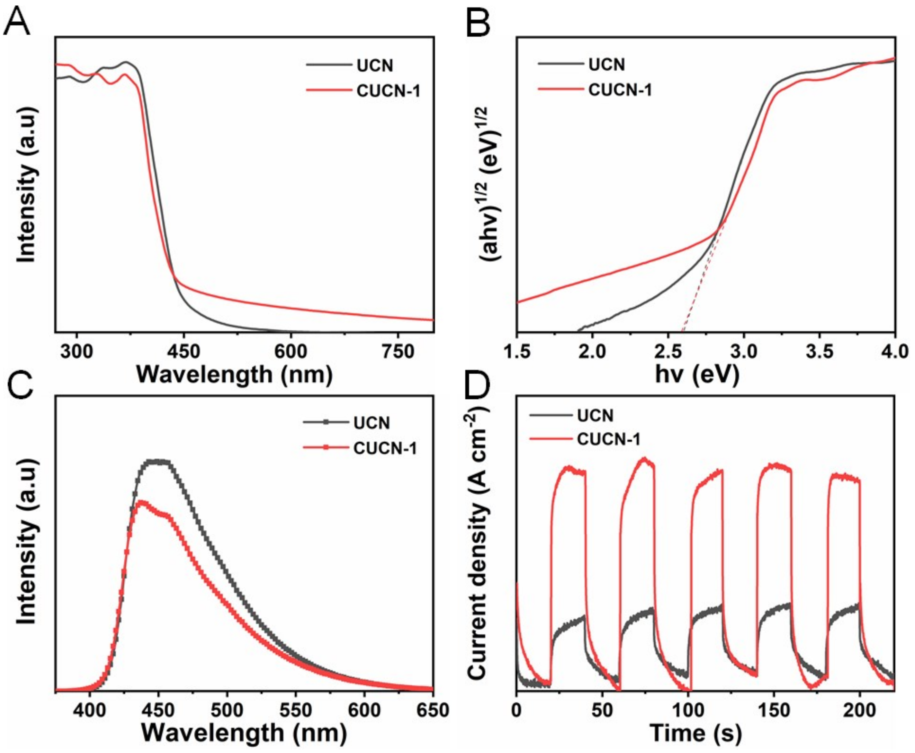

Figure S20. (A) UV-visible light absorption spectra; (B) The Tauc/Davis-Mott plots of UCN and CUCN-1; (C) the PL spectra of different samples; (D) transient photocurrent response.

Table S1. Surface element component of C, N and O calculated from XPS

Sample	C / mol%	N / mol%	O / mol%	C/N
MCN	45.14	52.60	2.26	0.85
CMCN	45.86	51.98	2.17	0.88

Table S2. Relative ratios of C-NH, N-(C)$_3$, C-N=C and the π-excitations determined by N1s spectra

Samples	N-H		N-(C)$_3$		C-N=C		the π-excitations	
	area	**%**	**area**	**%**	**area**	**%**	**area**	**%**
MCN	20351	9.31	49214	22.53	143006	65.43	5977	2.73
CMCN-1	18821	8.04	47342	20.22	162571	69.43	5401	2.31

Table S3. Relative ratios of N-C=N, C=C and C-NH determined by C1s spectra

Samples	**N-C=N**		**C=C**		**C-N**	
	area	**%**	**area**	**%**	**area**	**%**
MCN	88768	78.80	17577	15.60	6306	5.59
CMCN-1	95455	78.15	21641	17.72	5049	4.13

Table S4 Elemental analysis results of MCN and CMCN

Sample	N / mol%	C / mol%	H / mol%	C/N
MCN	45.75	29.47	24.78	0.64
CMCN	45.57	29.84	24.59	0.65

Table S5. The calculated Apparent Quantum Efficiency (AQE) of CMCN-1 at different wavelength.

Wavelength	H_2 Evolved	Irradiation power	AQE
420 nm	64.0 μmol	88.7 mW	3.8%
450 nm	33.7 μmol	71.1 mW	2.5%
500 nm	20.0 μmol	178.9 mW	0.7%

Table S6. The radiative fluorescence lifetimes and relative percentages of photogenerated charge carriers in MCN and CMCN-1.

Samples	τ_1/ns (rel.%)	τ_2/ns (rel.%)	τ_3/ns (rel.%)	τ/ns
MCN	3.25 (55.52)	12.25 (19.28)	0.80 (25.20)	2.41
CMCN-1	2.29 (54.64)	8.82 (16.91)	0.55 (28.45)	1.29

Table S7. Summary of the photocatalytic hydrogen evolution performance of g-C3N4 based catalysts

Catalyst	Cocatalyst	Sacrificial	Light source	H_2 rate	Ref.
CQD/g-C_3N_4	Pt, 3 wt %	Methanol 25 vol %	300 W Xe lamp λ>400nm	3538 μmol h^{-1} g^{-1}	6
N-doped g-C_3N_4	Pt, 3 wt %	Triethanolamine 10 vol %	300 W Xe lamp >420nm	1280 μmol h^{-1} g^{-1}	7
CCN	Pt, 3 wt %	Triethanolamine 10 vol %	300 W Xe lamp >420nm	529 μmol h^{-1} g^{-1}	8
Pt-CN	-	Triethanolamine 10 vol %	300 W Xe lamp (PLS-SXE300)	6360 μmol h^{-1} g^{-1}	9
C-PDA–g-C_3N_4	Pt, 1.5 wt %	Triethanolamine 10 vol %	300 W Xe lamp λ>400nm	811 μmol h^{-1} g^{-1}	10
CQDs/C_3N_4	Pt, 3 wt %	Bisphenol A	300 W Xe lamp >420nm	152 μmol h^{-1} g^{-1}	11
S-Pt-C3N4	Pt, 3 wt %	Triethanolamine 10 vol %	300 W Xenon lamp simulated solar light	14700 μmol h^{-1} g^{-1}	12
N-GQDs/CN-U	Pt, 1 wt %	Triethanolamine 15 vol %	300 W Xe lamp >420nm	2180 μmol h^{-1} g^{-1}	13
Ag/CQDs/g-C_3N_4	--	Triethanolamine 10 vol %	300 W Xe lamp >550nm	627 μmol h^{-1} g^{-1}	14
$W_{18}O_{49}$@g-C_3N_4	Pt, 1 wt %	Triethanolamine 10 vol %	300 W Xe lamp AM 1.5	1009 μmol h^{-1} g^{-1}	15
PCN-U	Pt, 3 wt %	Triethanolamine 10 vol %	300 W Xe lamp λ>400nm	5222 μmol h^{-1} g^{-1}	16
CNS-Pt	Pt, 1 wt %	Triethanolamine 10 vol %	350 W Xe lamp >420nm	4210.8 μmol h^{-1} g^{-1}	17
O-g-C_3N_4	Pt, 3 wt %	Triethanolamine 10 vol %	300 W Xe lamp λ>400nm	8874.7 μmol h^{-1} g^{-1}	18
O-g-C_3N_4	Pt, 3 wt %	Triethanolamine 10 vol %	300 W Xe lamp λ>420nm	350 μmol h^{-1} g^{-1}	18
m-CN-0.067	Pt, 0.5 wt %	Triethanolamine 15 vol %	300 W Xe lamp λ>420nm	2500 μmol h^{-1} g^{-1}	19
P-DCN	Pt, 3 wt %	Triethanolamine 10 vol %	300 W Xe lamp >420nm	2092 μmol h^{-1} g^{-1}	20
PFBT/CN	Pt, 1 wt %	Triethanolamine 10 vol %	300 W Xe lamp >420nm	722 μmol h^{-1} g^{-1}	21
Rh-P/CN(H)	Pt, 1 wt %	Triethanolamine	300 W Xe lamp	2075 μmol h^{-1} g^{-1}	22

Catalyst	Cocatalyst	Sacrificial	Light source	H_2 rate	Ref.
		10 vol %	>400nm		
$g\text{-}C_3N_4\text{-}MF_{100}$ D-A conjugated copolymer	Pt, 3 wt %	Triethanolamine 20 vol %	300 W Xe lamp >420nm	3612.65 μmol h^{-1} g^{-1}	[23]
Fe@g-C_3N_4	Pt, 3 wt %	Triethanolamine 10 vol %	300 W Xe lamp >420nm	3390 μmol h^{-1} g^{-1}	[24]
CMCN	Pt, 1 wt %	Triethanolamine 10 vol %	300 W Xe lamp >420nm	5549 μmol h^{-1} g^{-1}	This work
CUCN	Pt, 1 wt %	Triethanolamine 10 vol %	300 W Xe lamp >420nm	5265 μmol h^{-1} g^{-1}	This work

References:

1. G. Kresse and D. Joubert, *Phys. Rev. B*, 1999, **59**, 1758-1775.
2. G. Kresse and J. Hafner, *Phys. Rev. B*, 1993, **47**, 558-561.
3. G. Kresse and J. Furthmüller, *Phys. Rev. B*, 1996, **54**, 11169-11186.
4. J. P. Perdew, K. Burke and M. Ernzerhof, *Phys Rev Lett*, 1996, **77**, 3865-3868.
5. H. J. Monkhorst and J. D. Pack, *Phys. Rev. B*, 1976, **13**, 5188-5192.
6. Y. Wang, X. Liu, J. Liu, B. Han, X. Hu, F. Yang, Z. Xu, Y. Li, S. Jia, Z. Li and Y. Zhao, *Angew. Chem. Int. Ed.*, 2018, **57**, 5765-5771.
7. Y. Zhou, L. Zhang, W. Huang, Q. Kong, X. Fan, M. Wang and J. Shi, *Carbon*, 2016, **99**, 111-117.
8. H. Li, F. Li, Z. Wang, Y. Jiao, Y. Liu, P. Wang, X. Zhang, X. Qin, Y. Dai and B. Huang, *Appl. Catal. B: Environ.*, 2018, **229**, 114-120.
9. X. Li, W. Bi, L. Zhang, S. Tao, W. Chu, Q. Zhang, Y. Luo, C. Wu and Y. Xie, *Adv. Mater.*, 2016, **28**, 2427-2431.
10. F. He, G. Chen, Y. Yu, Y. Zhou, Y. Zheng and S. Hao, *Chem. Commun.*, 2015, **51**, 6824-6827.
11. G. Zhang, Q. Ji, Z. Wu, G. Wang, H. Liu, J. Qu and J. Li, *Adv. Funct. Mater.*, 2018, **28**, 1706462.
12. L. Zhang, R. Long, Y. Zhang, D. Duan, Y. Xiong, Y. Zhang and Y. Bi, *Angew. Chem. Int. Ed.*, 2020, **59**, 6224-6229.
13. J.-P. Zou, L.-C. Wang, J. Luo, Y.-C. Nie, Q.-J. Xing, X.-B. Luo, H.-M. Du, S.-L. Luo and S. L. Suib, *Appl. Catal. B: Environ.*, 2016, **193**, 103-109.
14. J. Qin and H. Zeng, *Appl. Catal. B: Environ.*, 2017, **209**, 161-173.
15. C. Feng, L. Tang, Y. Deng, J. Wang, Y. Liu, X. Ouyang, Z. Chen, H. Yang, J. Yu and J. Wang, *Appl. Catal. B: Environ.*, 2020, **276**, 119167.

16. P. Yang, H. Ou, Y. Fang and X. Wang, *Angew. Chem. Int. Ed.*, 2017, **56**, 3992-3996.
17. M. Liu, P. Xia, L. Zhang, B. Cheng and J. Yu, *ACS Sustain. Chem. Eng.*, 2018, **6**, 10472-10480.
18. X. She, J. Wu, J. Zhong, H. Xu, Y. Yang, R. Vajtai, J. Lou, Y. Liu, D. Du, H. Li and P. M. Ajayan, *Nano Energy*, 2016, **27**, 138-146.
19. J. Li, D. Wu, J. Iocozzia, H. Du, X. Liu, Y. Yuan, W. Zhou, Z. Li, Z. Xue and Z. Lin, *Angew. Chem. Int. Ed.*, 2019, **58**, 1985-1989.
20. D. Zhang, Y. Guo and Z. Zhao, *Appl. Catal. B: Environ.*, 2018, **226**, 1-9.
21. J. Chen, C. L. Dong, D. Zhao, Y. C. Huang, X. Wang, L. Samad, L. Dang, M. Shearer, S. Shen and L. Guo, *Adv. Mater.*, 2017, **29**, 1606198.
22. Z. Chen, Y. Bu, L. Wang, X. Wang and J.-P. Ao, *Appl. Catal. B: Environ.*, 2020, **274**, 119117.
23. H. Che, C. Liu, G. Che, G. Liao, H. Dong, C. Li, N. Song and C. Li, *Nano Energy*, 2020, **67**, 104273.
24. W. Zhang, Q. Peng, L. Shi, Q. Yao, X. Wang, A. Yu, Z. Chen and Y. Fu, *Small*, 2019, **15**, 1905166.